

Analysis of elastic, quasielastic, and inelastic scattering of lithium isotopes on a ^{28}Si target

B. Canbula,* D. Canbula, and H. Babacan

Department of Physics, Faculty of Arts and Sciences, Celal Bayar University, 45140, Muradiye, Manisa, Turkey

(Received 20 March 2015; published 21 April 2015)

The elastic and inelastic cross sections of ^6Li on ^{28}Si at 240 MeV, and quasielastic cross section of ^7Li and ^{11}Li on ^{28}Si at 177.8 and 319 MeV, respectively, are analyzed with the coupled-channels method. The collective nuclear level density is used to determine the deformation parameter regarding to the first-excited state of ^{28}Si . The results are in agreement with the experimental data and indicate the need of using a nuclear structure model such as nuclear level density to reduce the ambiguity between the optical model parameters and the deformation parameter. Additionally, the spin-orbit potential is found to have an important role in reproducing the data of the quasielastic scattering of ^7Li and ^{11}Li on a ^{28}Si target.

DOI: [10.1103/PhysRevC.91.044615](https://doi.org/10.1103/PhysRevC.91.044615)

PACS number(s): 24.10.Eq, 25.60.Bx, 21.10.Ma, 21.10.Re

I. INTRODUCTION

The lightest metal, lithium, has always been of interest for both experimental and theoretical nuclear physicists with its weakly bound isotopes. Since ^6Li and ^7Li have 1.47 MeV and 2.46 MeV deuteron and triton separation energies, respectively, they have been considered as binary clusters. Thus, the breakup and transfer mechanisms for these isotopes are of crucial importance [1,2]. ^6Li is also subject of many studies aiming to build a bridge between the elastic scattering of light and heavy ions because it is the lightest heavy-ion projectile [3]. The measurements of elastic scattering angular distributions of ^6Li and ^7Li have been performed for more than fifty years [3–13]. Especially for ^6Li , there are enough data even for investigation of the mass number and energy dependence of the optical model parameters [14–16]. However, for ^7Li , the corresponding experimental data are very scarce [2,4,13,17–19]. Additionally, unexpected energy dependence of the optical model parameters around the Coulomb barrier; namely, threshold anomaly, have been also widely studied for ^6Li and ^7Li [2,11,19–21].

On the other hand, light exotic nuclei such as ^{11}Li around the neutron and proton driplines have some phenomenal characteristic properties such as high root-mean-square (rms) values, low nuclear matter densities, low binding energies, etc. After the 1980s, for studying these nuclei, an opportunity has arisen with the use of radioactive ion beams (RIBs) [22,23]. Then, it was shown that some of these nuclei consist of a hard core and weakly bound neutron(s) or proton(s), which are called a halo structure. ^{11}Li is the one of the two well-known neutron halo nuclei with its two-neutron separation energy of 0.363 MeV. Moreover, since ^{10}Li and $2n$ binary systems are unbound, ^{11}Li has a three-body structure known as Borromean. With all these extraordinary properties, the halo nucleus ^{11}Li has become an interesting subject of nuclear physics and the number of both theoretical and experimental studies about it has been drastically increased [18,24–27]. With these experimental studies, a huge experimental database has been built, which includes many unexplained data still waiting to reproduce theoretically.

Weakly-bound-nuclei-induced reactions on light-mass targets, such as ^{12}C , ^{16}O , ^{24}Mg , ^{27}Al , and ^{28}Si , are well-established tools to investigate the nuclear breakup effects [1,2,13,21,28,29]. Thus, as a first step, elastic scattering of these nuclei should be described precisely. However, since a weakly bound nucleus has too many low- $|Q|$ reaction channels, the energy resolution of the detectors is usually not enough to separate inelastic contributions for obtaining pure elastic cross sections. Therefore, describing the elastic scattering of a weakly bound nucleus is more challenging compared to that of a stable nucleus. This type of cross sections (including some inelastic contributions) are known as quasielastic and can be calculated by using the coupled-channels (CC) method. With this method the inelastic scattering to the low-lying collective states of the projectile or target can be described by means of the corresponding deformation parameters. When pure elastic- and inelastic-cross-section data exist separately, the optical-potential parameters are adjusted to the pure elastic data and then the deformation parameter is adjusted to accurately reproduce the inelastic data. But, for the quasielastic data, there is an ambiguity in determining the optical potential and the deformation parameters simultaneously. Thus, the value of the deformation parameter should be determined from a nuclear structure model. Recently, we proposed a new method, which gives the deformation parameter values from the energy of the excited states by using the collective nuclear level density [30].

In the light of the above considerations, in this paper, we aim to analyze the elastic, quasielastic, and inelastic scattering cross sections of the lithium isotopes ^6Li , ^7Li , and ^{11}Li on a ^{28}Si target. ^{28}Si is selected because the cross-section data are available for most of the lithium isotopes. For this purpose, we perform CC calculations to take into account the inelastic contributions by using the deformation parameter of the first-excited state of ^{28}Si , which is predicted by using the collective nuclear level density [30]. We worked out these calculations in two steps. First, we test our prediction for the deformation parameter of ^{28}Si in the inelastic scattering of ^6Li on a ^{28}Si target at 240 MeV, whose elastic and inelastic cross sections were measured by Chen *et al.* [12]. Next, we use the same value of the deformation parameter in analyzing the quasielastic scattering of ^7Li and ^{11}Li on a ^{28}Si target at 177.8

*bora.canbula@cbu.edu.tr

and 319 MeV, respectively, both measured by Lewitowicz *et al.* [18].

The elastic and inelastic data presented by Chen *et al.* [12] are relatively new and have not yet been extensively investigated. The first analysis was performed by Chen *et al.* themselves [12] by using the optical model with a phenomenological Woods–Saxon potential and the folding model with M3Y and JLM effective nucleon-nucleon interactions. The same group also tested a systematic optical potential in another paper [31] to describe the elastic scattering of ${}^6\text{Li}$ on targets $24 \geq A \geq 90$ at 240 MeV. Finally, Kim *et al.* [32] used the eikonal model to analyze these data. However, these studies aimed to reproduce the elastic-scattering cross section without any additional effort to describe the inelastic scattering. This study, however, focuses on analyzing the inelastic scattering of ${}^6\text{Li}$ on ${}^{28}\text{Si}$ at 240 MeV.

Lewitowicz *et al.* [18] measured the quasielastic scattering of ${}^7\text{Li}$ and ${}^{11}\text{Li}$ on a ${}^{28}\text{Si}$ target at 178 and 319 MeV, respectively. They analyzed their data by CC calculations by using the phenomenological Woods–Saxon potential and also the folding potential with the M3Y effective nucleon-nucleon interaction. It is mentioned in Ref. [18] that only the 2^+ state of ${}^{28}\text{Si}$ is included in the analyses because it was found that the contribution of higher states is at least one order of magnitude smaller than that of the 2^+ state and therefore can be neglected [9]. However, a strong modification of the optical-potential parameters or a large renormalization of the folding potential is needed to reproduce the data. In the following years, many different approaches were proposed to explain these data. One of them was performed by Al-Khalili [29]. He studied the breakup effects on the elastic scattering of ${}^{11}\text{Li}$ from ${}^{28}\text{Si}$ by using a four-body Glauber model but was not able to reproduce the cross-section data. A better, but still unsatisfactory, agreement is obtained by Cooper and Mackintosh [33] with a two-step phenomenology, in which $S(l)$ is adjusted to data and $V(r)$ is produced by inversion of $S(l)$. In another attempt to describe this quasielastic scattering, Fayans *et al.* [34] used a folding potential based on the M3Y effective nucleon-nucleon interaction. However, they could not reproduce the oscillation of the experimental values. Carstoiu and Lassaut [35] tried to find a consistent description for the scattering of both ${}^6\text{Li}$ and ${}^{11}\text{Li}$ on ${}^{12}\text{C}$ and ${}^{28}\text{Si}$ targets. They used the M3Y and JLM interactions in the folding model and succeeded to reproduce the ${}^{12}\text{C}$ data but sufficient agreement was not achieved for ${}^{28}\text{Si}$. A similar agreement was also obtained by Rashdan [36] within relativistic mean-field theory. Furthermore, a fitted polarization potential together with the folding model was tried by Pacheco and Vinh Mau [37], but it was not able to reproduce the data. Finally, Un *et al.* [38] showed that modifying the shape of the both the real and imaginary potentials in the surface region leads to an improvement in the agreement between the predictions and the data. However, it still remains a great challenge to describe the quasielastic scattering of ${}^{11}\text{Li}$ on ${}^{28}\text{Si}$ and it seems that the only possible way to solve this problem is to strengthen the connection between the reaction and the structure.

This paper is organized as follows: In Sec. II, we briefly outline the methods used in our calculations. In Sec. III, we

present our results and their implications. Finally in Sec. IV, we give some concluding remarks.

II. THEORY

A. Optical model and coupled-channels method

Describing the interaction between the projectile and target is a complicated problem that has not yet been solved. One way to overcome this many-body problem is to use the optical model. The optical model defines the interaction by an effective potential that consists of some potentials terms such as the volume term

$$V_{\text{Vol}}(r) = \frac{V_0}{1 + \exp\left(\frac{r-R_v}{a_v}\right)} + \frac{iW_0}{1 + \exp\left(\frac{r-R_w}{a_w}\right)}, \quad (1)$$

a derivative surface term

$$V_{\text{Sur}}(r) = 4a_{\text{vd}}V_d \frac{d}{dr} \frac{1}{1 + \exp\left(\frac{r-R_{\text{vd}}}{a_{\text{vd}}}\right)} + 4ia_{\text{wd}}W_d \frac{d}{dr} \frac{1}{1 + \exp\left(\frac{r-R_{\text{wd}}}{a_{\text{wd}}}\right)}, \quad (2)$$

a spin-orbit term

$$V_{\text{so}}(r) = \left(\frac{\hbar}{m_\pi c}\right)^2 \frac{1}{r} \left[\frac{d}{dr} \frac{V_{\text{so}}}{1 + \exp\left(\frac{r-R_{\text{vso}}}{a_{\text{vso}}}\right)} + \frac{d}{dr} \frac{iW_{\text{so}}}{1 + \exp\left(\frac{r-R_{\text{wso}}}{a_{\text{wso}}}\right)} \right] 2\mathbf{L} \cdot \mathbf{s}, \quad (3)$$

where $(\hbar/m_\pi c)^2 = 2 \text{ fm}^2$, and a Coulomb term

$$V_c(r) = \begin{cases} \frac{Z_P Z_T e^2}{2R_c} \left(3 - \frac{r^2}{R_c^2}\right), & r \leq R_c \\ \frac{Z_P Z_T e^2}{r}, & r \geq R_c, \end{cases} \quad (4)$$

under the uniformly-charged-sphere assumption. The radius parameters are defined as

$$R_i = r_i (A_P^{1/3} + A_T^{1/3}), \quad (5)$$

where P , T , and i indicate the projectile, target, and the type of the potential, respectively. Elastic-scattering data are used to determine the optical model parameters V_i , W_i , r_i , and a_i by minimizing a χ^2 function, which is defined as

$$\chi^2 = \sum_{i=1}^N \left[\frac{\sigma_{\text{theor}}(\theta_i) - \sigma_{\text{expt}}(\theta_i)}{\Delta\sigma_{\text{expt}}(\theta_i)} \right]^2, \quad (6)$$

for N data points at angles θ_i . $\sigma(\theta_i)$ corresponds to predicted and experimental cross sections and its error.

To calculate the quasielastic or inelastic cross section, the coupled-channels method is the most widely used and a very well tested extension of the optical model. With this method, one can describe the collective inelastic excitations of the target or projectile by deforming the optical potential. To define the deformed surface of a nucleus, which causes a rotational excitation, spherical harmonics $Y_L^M(\theta, \phi)$ can be used as

$$R(\theta, \phi) = R_0 + \sum_{L,M} \delta_{L,M} Y_L^M(\theta, \phi), \quad (7)$$

where θ and ϕ are the polar angles, R_0 is the average surface radius, and $\delta_{L,M}$ are the deformation lengths. The $L = 0$ and $L = 1$ cases do not have any contribution, therefore, the sum starts from $L = 2$, which corresponds to quadrupole deformations. Additionally, for an axially deformed nucleus, only $M = 0$ is taken into account. Therefore, the deformed optical potential is given by

$$U(r, \theta, \phi) = U(r) - \sum_{L=2} \delta_L Y_L^0(\theta, \phi) \frac{dU(r)}{dr}, \quad (8)$$

where $U(r)$ is the effective potential, which is defined as

$$U(r) = V_{\text{Vol}}(r) + V_{\text{Sur}}(r) + V_{\text{so}}(r) + V_c(r). \quad (9)$$

Deformation lengths can be expressed as

$$\delta_L = \beta_L R_0 \quad (10)$$

in terms of the deformation parameters β_L . The values of the deformation parameter can be determined from the inelastic-scattering data when they exist separately. However, for describing the quasielastic data, there would be an ambiguity between the optical model parameters and the deformation parameter. Therefore, the most reliable way to determine the deformation parameter would be to obtain its value from a nuclear structure model. Such a model is presented in the following section.

B. Nuclear level density

The need of a nuclear structure model to obtain the value of the deformation parameter to use in coupled-channels method is especially revealed in the lack of inelastic-scattering data. Therefore, the structure model to be used in calculations should be able to fix the value of the deformation parameter from a structural feature of the nucleus, which could exist for any nuclei. The energy of excited levels E_i can be considered as the most fundamental among them and can be related with the number of excited levels as

$$1, 2, 3, \dots = \int_0^{E_{1,2,3,\dots}} \rho^{\text{tot}}(U, a) dU, \quad (11)$$

where ρ^{tot} is the total nuclear level density as a function of excitation energy U and the level density parameter a . Nuclear level density (NLD) is defined as the number of excited levels around an excitation energy and is given as

$$\rho^{\text{tot}}(U, a) = \frac{1}{12\sqrt{2}\sigma} \frac{\exp[2\sqrt{aU}]}{a^{1/4}U^{5/4}}, \quad (12)$$

according to the well-known Fermi gas model [40]. $\sigma^2 = TI/\hbar^2$ is known as the spin cutoff parameter and is defined in terms of the nuclear temperature $T = \sqrt{U/a}$ and the moment of inertia I . The dependence of NLD on the deformation parameter is provided by the Laplace-like formula of the level density parameter [30]

$$a(U, \beta) = \tilde{a} \left(1 + A_c(\beta) \frac{S_n \exp(-|U - E_0|/\sigma_c'^3)}{\sigma_c'^3} \right), \quad (13)$$

where S_n is the neutron separation energy and $E_0 = 0.2\hbar\omega$ is the first-phonon-state energy [41]. The scale parameter $\sigma_c'^3 = \sigma_c^3/\tilde{a}$ is related with the spin cutoff parameter at a critical temperature $T_c = \sqrt{S_n/\tilde{a}}$. The collective amplitude A_c introduces the shape (and thus the deformation) dependency to the level density parameter and is given as follows:

$$A_c = [M_{\text{expt}}(N, Z) - M_{\text{LDM}}(N, Z, \beta)] \frac{\tau_c}{\sinh \tau_c}, \quad (14)$$

where $\tau_c = 2\pi^2 T_c/\hbar\omega$. M_{expt} is the experimental mass of the nucleus and M_{LDM} is the calculated mass of the deformed nucleus with the finite-range liquid-drop model [42],

$$M_{\text{LDM}}(N, Z, \beta) = M_0 + E \left(\frac{\alpha}{\alpha_0} \right)^2, \quad (15)$$

where M_0 is the calculated mass of the spherical nucleus having the same N and Z with the deformed nucleus. The ratio α/α_0 is the deformation magnitude and is given in terms of the deformation parameter as $\alpha^2 = (5/4\pi)\beta^2$ (see details of LDM in Ref. [42]). Furthermore, the asymptotic level density parameter \tilde{a} can also be calculated by taking into account the deformation of the nucleus [43]. However, in this study we employ the following definition using the shell correction $S(N, Z) = M_{\text{expt}}(N, Z) - M_{\text{LDM}}(N, Z, \beta = 0)$ and the pairing correction $\Delta = \pm 12/\sqrt{A}$:

$$\tilde{a} = \frac{\pi^2}{6} \sum_{i=p,n} g_i [E_F^i + S(N, Z) - \Delta], \quad (16)$$

where g is the single-particle level density and E_F is the Fermi energy [30].

III. RESULTS AND DISCUSSION

In the calculation of the elastic, quasielastic and inelastic cross sections of lithium isotopes on a ^{28}Si target, we use the optical model parameters and the deformation parameter of the first-excited state of ^{28}Si . It is predicted as -0.362 by inverting the relation (11) between the excitation energy and the cumulative number of excited levels up to this energy. Following such a method also gives us the energy of the first-excited state as a function of deformation parameter, which is given in Fig. 1. The energy of the first-excited state of ^{28}Si is increasing with the deformation parameter. The value of -0.362 is fixed by using 1.78 MeV for the experimental value of the first-excited state. It is already shown that ^{28}Si is a well-deformed nucleus with electron-scattering experiments [44], and our prediction is in agreement with the previous estimations performed with the coupled-channels method [8,45,46]. This value is also consistent with the ground-state deformation of ^{28}Si given in RIPL-3 mass tables [47]. Our prediction for the deformation parameter is about 10% smaller than the values obtained from the measured quadrupole moment [48] and reduced electric quadrupole transition probability [49]. This difference could be due to the larger values of the deformation parameter is for the electromagnetic transition, while our prediction applies to

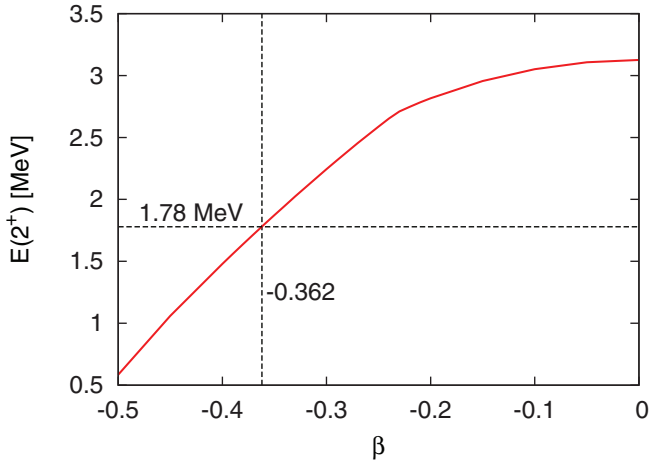


FIG. 1. (Color online) The energy of the first-excited state of ^{28}Si as a function of deformation parameter.

the isoscalar excitation. However, there are some other studies suggesting a larger deformation parameter [50].

The most straightforward way to test our prediction on the deformation parameter is to use it in a coupled-channels analysis. First, we choose the scattering of ^6Li on ^{28}Si at 240 MeV because there exist both elastic- and inelastic-cross-section data for this system [12]. Therefore, there would be no ambiguity between the optical model parameters and the deformation parameter. We use the same optical model parameters as those given in Ref. [12] without any further adjustments, which provides a sensitive test for our prediction. This optical model potential could also simulate the continuum breakup effects in the elastic scattering of ^6Li , which are shown to be very important with a recent continuum-discretized coupled-channels (CDCC) analysis [51]. The calculation of elastic and inelastic cross sections for $^6\text{Li} + ^{28}\text{Si}$ at 240 MeV are performed with FRESKO [52] using the optical model parameters given in Table I. The results are shown in Fig. 2. It is seen from the lower panel of the figure that the deformation parameter obtained by using our collective nuclear level density formulation [30] describes the inelastic-cross-section data very well. Therefore, this promising result leads us to use our prediction in a more challenging problem, which has remained unexplained so far [18].

Next, a coupled-channels analysis of the quasielastic scattering of ^7Li on ^{28}Si is performed. In order to present a

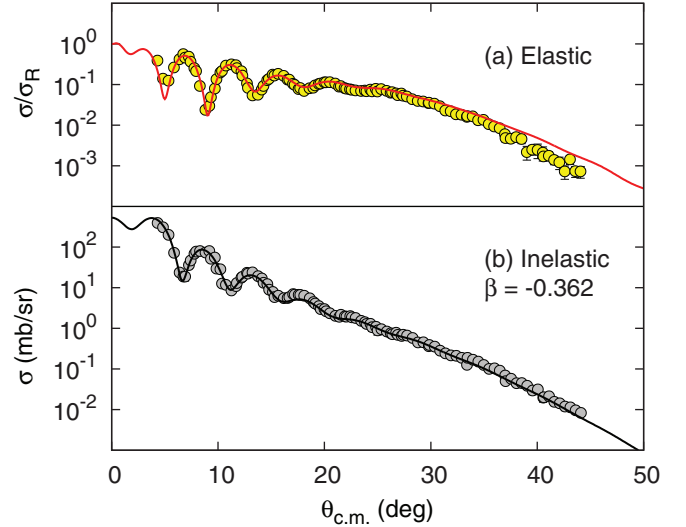


FIG. 2. (Color online) Angular distribution of the elastic (upper panel) and inelastic (lower panel) cross section for $^6\text{Li} + ^{28}\text{Si}$ scattering at 240 MeV. The experimental data are taken from Chen *et al.* [12].

consistent analysis and minimize the uncertainties arising from the optical model parameters, we define ^7Li as a two-body system consisting of a valence neutron coupled to ^6Li core. Since the experimental data were measured at 177.8 MeV, we need the optical model parameters for $n + ^{28}\text{Si}$ elastic scattering at 25.4 MeV. Moreover, we still need to slightly modify the optical model parameters of $^6\text{Li} + ^{28}\text{Si}$ system. There is not any measurement of the elastic scattering of n on a ^{28}Si target at 25.4 MeV, which can be used to determine the optical model parameters. Therefore, we rely on a global optical potential [39]. We test the validation of this global potential by performing calculations at 15.4, 18.9 and 21.7 MeV for which the experimental data exist [53,54]. The results are shown in Fig. 3. It seems that the global optical potential of Koning and Delaroche [39] is very reliable to describe the elastic scattering of n on a ^{28}Si target at the considered energy range. Therefore, we employ the optical model parameters obtained from this global parametrization and only modify the real and imaginary depths of $^6\text{Li} + ^{28}\text{Si}$ potential to 143.4 and 35.60 MeV, respectively. The results are shown in Fig. 4 with the blue solid line. The gray dotted line represents the coupled-channels calculation with the

TABLE I. Optical model parameters for given interactions. The Coulomb radius parameter r_c is taken as 1.20 fm for all interactions.

Potential	Type	V_i MeV	r_i fm	a_i fm	W_i MeV	r_i fm	a_i fm
$^6\text{Li} + ^{28}\text{Si}$ [12]	Volume	143.34	0.720	0.937	32.13	1.004	0.921
$n + ^{28}\text{Si}$ [39]	Volume	44.67	1.170	0.668	2.58	1.170	0.668
	Surface				5.57	1.294	0.540
	Spin-orbit	5.15	1.000	0.580	0.17	1.000	0.580
$^7\text{Li} + ^{28}\text{Si}$	Volume	138.50	0.587	0.790	32.04	1.106	0.884
	Spin-orbit	5.036	0.587	0.790	0.783	1.106	0.884
$^{11}\text{Li} + ^{28}\text{Si}$	Volume	143.34	0.838	0.937	32.13	1.004	0.876
	Spin-orbit	2.002	0.838	0.937	0.581	1.004	0.876

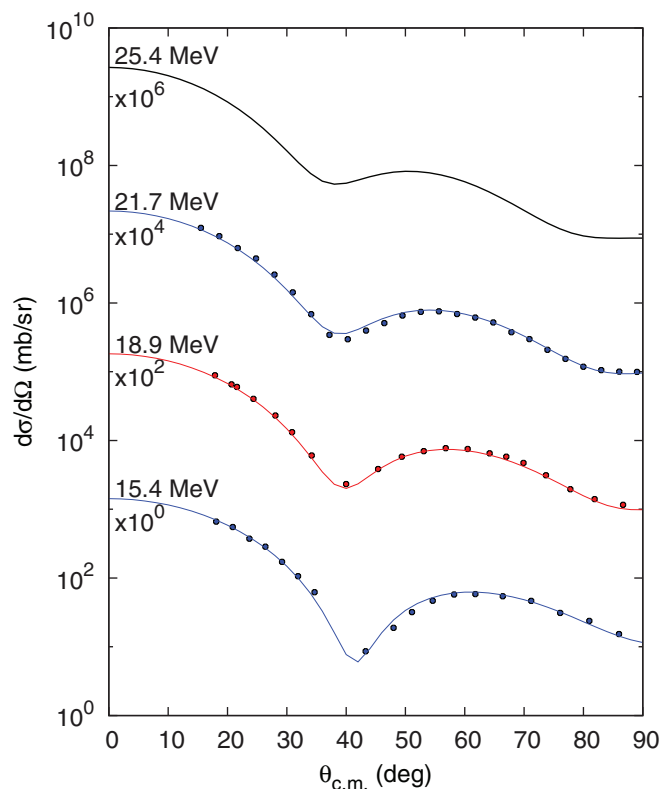


FIG. 3. (Color online) Angular distribution of the elastic cross section for $n + {}^{28}\text{Si}$ scattering at 15.4, 18.9, 21.7, and 25.4 MeV compared with the experimental data [53,54].

double-folding model using the DDM3Y interaction, which is performed by Lewitowicz *et al.* themselves [18]. As seen from figure, both our two-body model of ${}^7\text{Li}$ and the double-folding model are far from reproducing the quasielastic-scattering data. Therefore, we expand our investigation to include the search of optical model parameters. We use the potential of ${}^6\text{Li} + {}^{28}\text{Si}$ as the initial set of parameters and continue to modify until the minimum χ^2 is reached. However, modifying

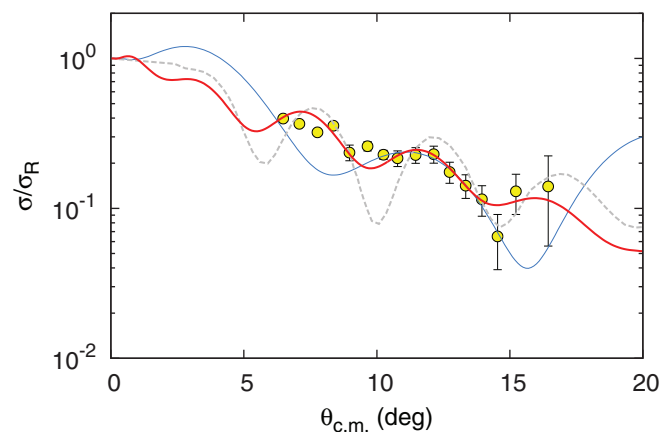


FIG. 4. (Color online) Angular distribution of the quasielastic cross section for ${}^7\text{Li} + {}^{28}\text{Si}$ scattering at 177.8 MeV. The experimental data are taken from Lewitowicz *et al.* [18].

only the volume potential is not sufficient to describe the quasielastic data, but a small spin-orbit potential with the same geometry improves the fit very significantly. The fitted optical potential parameters are given in Table I and the cross section results using these parameters are shown with the red solid line in Fig. 4. Our coupled-channels calculation with an optical model potential including volume and spin-orbit terms combined with our deformation-parameter prediction for inelastic contributions seems to be much better compared with other approaches.

Finally, the quasielastic scattering of ${}^{11}\text{Li}$ on a ${}^{28}\text{Si}$ target at 319 MeV is investigated. Although it is highly desired to define ${}^{11}\text{Li}$ with a three-body model consisting of two valence neutrons and a ${}^9\text{Li}$ core, there are no experimental data for ${}^9\text{Li} + {}^{28}\text{Si}$ elastic scattering. Therefore, the interaction potential between ${}^9\text{Li}$ and ${}^{28}\text{Si}$ could not be deduced. Considering that almost all possible methods have already been applied [18,29,33–38] to this problem, we try to reproduce these data by using the coupled-channels method with the predicted deformation parameter of ${}^{28}\text{Si}$ and an optical model potential including volume and spin-orbit terms, similar to ${}^7\text{Li}$. The corresponding optical model parameters are given in Table I and the results are displayed in Fig. 5. The red solid line and the gray dotted line represent our results and the results taken from Ref. [38], respectively. The results of Ref. [38] are selected for comparison because of their good agreement with the experimental data. It seems that our calculation also agrees quite well with the experimental data, especially for a simple optical model potential.

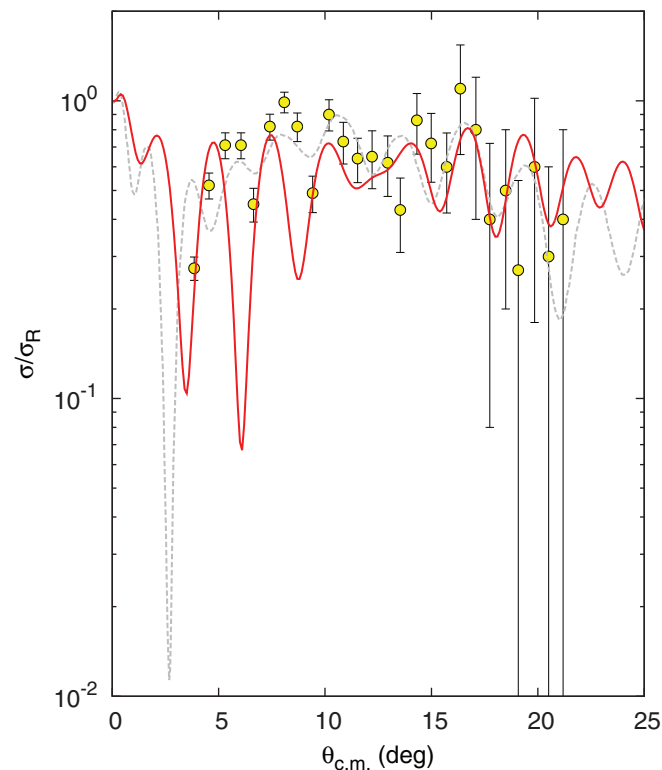


FIG. 5. (Color online) Angular distribution of the quasielastic cross section for ${}^{11}\text{Li} + {}^{28}\text{Si}$ scattering at 319 MeV. The experimental data are taken from Lewitowicz *et al.* [18].

IV. CONCLUSIONS

In summary, we analyzed the elastic-, inelastic-, and quasielastic-scattering cross-section data of the projectiles ^6Li , ^7Li , and ^{11}Li on a ^{28}Si target at 240 MeV [12], 177.8 MeV [18], and 319 MeV [18], respectively, by using the coupled-channels method. For the inelastic contributions, the deformation parameter of the first-excited state of ^{28}Si is obtained by using the recently proposed collective nuclear level density formulation [30]. The following concluding remarks can be drawn from this study:

- (i) The nuclear level density is used to determine the deformation parameter of an excited state to be used in coupled-channels method.
- (ii) The predicted deformation parameter for the first-excited state of ^{28}Si is in agreement with the previous studies [8,45–47]. It is also tested in the inelastic-scattering cross section calculation of ^6Li on ^{28}Si at 240 MeV for comparison with experimental data [12] and is proven to be accurate.

- (iii) The same value of the deformation parameter obtained from our NLD formulation is used in the analysis of the quasielastic-cross-section data [18] of ^7Li and ^{11}Li on ^{28}Si to obtain the optical model parameter sets. These results suggest that the spin-orbit potential has a very crucial role to reproduce the data. Therefore, to strengthen the connection between the nuclear structure and reaction calculations reduces the ambiguity between the optical model parameters and the deformation parameter and thus may help significantly to solve some challenging reaction problems.

- (iv) Finally, our collective nuclear level density formulation [30] could be considered as a reliable and useful tool to determine the deformation parameter to be used in a coupled-channels analysis.

ACKNOWLEDGMENTS

This work was supported by the Turkish Science and Research Council (TÜBİTAK) under Grant No. 112T566.

-
- [1] A. Pakou *et al.*, *Phys. Rev. Lett.* **90**, 202701 (2003).
 - [2] K. Zerva *et al.*, *Phys. Rev. C* **82**, 044607 (2010).
 - [3] P. Schwandt, W. W. Jacobs, M. D. Kaitchuck, P. P. Singh, W. D. Ploughe, F. D. Becchetti, and J. Jänecke, *Phys. Rev. C* **24**, 1522 (1981).
 - [4] K. Bethge, C. Fou, and R. Zurmühle, *Nucl. Phys. A* **123**, 521 (1969).
 - [5] R. M. DeVries, D. A. Goldberg, J. M. Watson, M. S. Zisman, and J. G. Cramer, *Phys. Rev. Lett.* **39**, 450 (1977).
 - [6] P. Schwandt, S. Kailas, W. W. Jacobs, M. D. Kaitchuck, W. Ploughe, and P. P. Singh, *Phys. Rev. C* **21**, 1656(R) (1980).
 - [7] J. Cook, H. Gils, H. Rebel, Z. Majka, and H. Klewe-Nebenius, *Nucl. Phys. A* **388**, 173 (1982).
 - [8] M. Vineyard, J. Cook, and K. Kemper, *Nucl. Phys. A* **405**, 429 (1983).
 - [9] A. Nadasen, M. McMaster, M. Fingal, J. Tavormina, P. Schwandt, J. S. Winfield, M. F. Mohar, F. D. Becchetti, J. W. Jänecke, and R. E. Warner, *Phys. Rev. C* **39**, 536 (1989).
 - [10] A. Nadasen *et al.*, *Phys. Rev. C* **47**, 674 (1993).
 - [11] A. Pakou *et al.*, *Phys. Lett. B* **556**, 21 (2003).
 - [12] X. Chen, Y.-W. Lui, H. L. Clark, Y. Tokimoto, and D. H. Youngblood, *Phys. Rev. C* **80**, 014312 (2009).
 - [13] M. Sinha, S. Roy, P. Basu, H. Majumdar, S. Santra, V. Parkar, K. Golda, and S. Kailas, *EPJ Web Conf.* **17**, 03004 (2011).
 - [14] J. Cook, *At. Data Nucl. Data Tables* **26**, 19 (1981).
 - [15] J. Cook, *Nucl. Phys. A* **375**, 238 (1982).
 - [16] J. Cook, *Nucl. Phys. A* **388**, 153 (1982).
 - [17] P. Schumacher, N. Ueta, H. Duhm, K.-I. Kubo, and W. Klages, *Nucl. Phys. A* **212**, 573 (1973).
 - [18] M. Lewitowicz *et al.*, *Nucl. Phys. A* **562**, 301 (1993).
 - [19] A. Pakou *et al.*, *Phys. Rev. C* **69**, 054602 (2004).
 - [20] M. A. Tiede, D. E. Trcka, and K. W. Kemper, *Phys. Rev. C* **44**, 1698 (1991).
 - [21] A. G. Camacho, P. R. S. Gomes, and J. Lubian, *Phys. Rev. C* **82**, 067601 (2010).
 - [22] I. Tanihata *et al.*, *Phys. Rev. Lett.* **55**, 2676 (1985).
 - [23] I. Tanihata *et al.*, *Phys. Lett. B* **160**, 380 (1985).
 - [24] J. Kolata *et al.*, *Phys. Rev. Lett.* **69**, 2631 (1992).
 - [25] M. C. Mermaz, *Phys. Rev. C* **47**, 2213 (1993).
 - [26] G. Bertsch, H. Esbensen, and A. Sustich, *Phys. Rev. C* **42**, 758 (1990).
 - [27] I. J. Thompson, J. S. Al-Khalili, J. A. Tostevin, and J. M. Bang, *Phys. Rev. C* **47**, R1364(R) (1993).
 - [28] G. Marti *et al.*, *Phys. Rev. C* **71**, 027602 (2005).
 - [29] J. Al-Khalili, *Nucl. Phys. A* **581**, 315 (1995).
 - [30] B. Canbula, R. Bulur, D. Canbula, and H. Babacan, *Nucl. Phys. A* **929**, 54 (2014).
 - [31] Krishichayan, X. Chen, Y.-W. Lui, J. Button, and D. H. Youngblood, *Phys. Rev. C* **81**, 044612 (2010).
 - [32] Y. J. Kim, J.-K. Woo, and S. J. Lee, *J. Korean Phys. Soc.* **60**, 1477 (2012).
 - [33] S. Cooper and R. Mackintosh, *Nucl. Phys. A* **582**, 283 (1995).
 - [34] S. Fayans, O. Knyazkov, I. Kuchkina, Y. E. Penionzhkevich, and N. Skobelev, *Phys. Lett. B* **357**, 509 (1995).
 - [35] F. Carstoiu and M. Lassaut, *Nucl. Phys. A* **597**, 269 (1996).
 - [36] M. Rashdan, *Phys. Rev. C* **54**, 315 (1996).
 - [37] J. Pacheco and N. Vinh Mau, *Nucl. Phys. A* **669**, 135 (2000).
 - [38] A. Un, Y. Kucuk, T. Caner, and I. Boztosun, *Phys. Rev. C* **89**, 057605 (2014).
 - [39] A. Koning and J. Delaroche, *Nucl. Phys. A* **713**, 231 (2003).
 - [40] H. A. Bethe, *Rev. Mod. Phys.* **9**, 69 (1937).
 - [41] A. Bohr and B. R. Mottelson, *Nuclear Structure* (World Scientific, Singapore, 1998), Vol. 1.
 - [42] W. D. Myers and W. J. Swiatecki, *Nucl. Phys.* **81**, 1 (1966).
 - [43] B. Canbula, R. Bulur, D. Canbula, and H. Babacan, *Eur. Phys. J. A* **50**, 178 (2014).
 - [44] A. Nakada and Y. Torizuka, *J. Phys. Soc. Jpn.* **32**, 1 (1972).
 - [45] H. Rebel, G. Schweimer, G. Schatz, J. Specht, R. Löhken, G. Hauser, D. Habs, and H. Klewe-Nebenius, *Nucl. Phys. A* **182**, 145 (1972).
 - [46] A. Obst and K. Kemper, *Phys. Rev. C* **6**, 1705 (1972).
 - [47] R. Capote *et al.*, *Nucl. Data Sheets* **110**, 3107 (2009).

- [48] N. J. Stone, *At. Data Nucl. Data Tables* **90**, 75 (2005).
- [49] S. Raman, C. Nestor, and P. Tikkanen, *At. Data Nucl. Data Tables* **78**, 1 (2001).
- [50] I. Boztosun and W. D. M. Rae, *Phys. Rev. C* **65**, 024603 (2002).
- [51] A. Gómez Camacho, A. Diaz-Torres, P. R. S. Gomes, and J. Lubian, *Phys. Rev. C* **91**, 014607 (2015).
- [52] I. J. Thompson, *Comput. Phys. Rep.* **7**, 167 (1988).
- [53] M. A. Al-Ohali, J. P. Delaroche, C. R. Howell, M. M. Nagadi, A. A. Naqvi, W. Tornow, R. L. Walter, and G. J. Weisel, *Phys. Rev. C* **86**, 034603 (2012).
- [54] R. Alarcon and J. Rapaport, *Nucl. Phys. A* **458**, 502 (1986).